

Seismic Reliability Analyses of Timber-Steel-Hybrid System

Xiaoyue Zhang

Graduate Student, Dept. of Wood Science, University of British Columbia, Vancouver, Canada

Michael Fairhurst

Graduate Student, Dept. of Civil Engineering, University of British Columbia, Vancouver, Canada

Thomas Tannert

Assistant Professor, Dept. of Civil Engineering, University of British Columbia, Vancouver, Canada

ABSTRACT: Reliability analyses are of great importance in performance-based seismic structural design as there are inherent uncertainties in both the actions (earthquakes) and the reactions (properties of the structural systems). In this paper, reliability analyses are performed on the “Finding the Forest Through the Trees” (FFTT) system, a novel timber-steel hybrid system. The FFTT system utilizes engineered timber products to resist gravity and lateral loads with interconnecting steel members to provide the necessary ductility for seismic demands. An improved response surface method with importance sampling is used to perform reliability-based seismic analyses. Peak inter-storey drift is selected as the main performance criterion as it is typically an indicator of overall damage to the structure. Uncertainties involving ground motions, weight (mass), stiffness and connection properties of the lateral load resisting system are considered in formulating the performance functions. A series of nonlinear dynamic analyses is run to generate the response database and the reliability index is evaluated using first-order reliability method (FORM) and importance sampling (IS) methods. The results show that the ductility reduction factor does not significantly influence the reliability index, while the structural weight and the hold-down stiffness play significant roles.

1. INTRODUCTION

Seismic reliability analyses should consider all required uncertainties to provide the most comprehensive safety assessment of a structure. These uncertainties involve the characteristic of the ground motions (e.g. peak ground accelerations, frequency contents, duration of shaking, etc.), the weight (e.g. dead loads and live loads), the material properties (e.g. strength and stiffness), and the connection properties (e.g. strength, stiffness, ductility) amongst others [1].

Reliability analyses form the basis of new “Performance-Based Design Guidelines” and allow introducing quality control procedures in the design process. Using reliability-based procedures, novel structural systems that are not covered by building codes can be designed to be as “safe” or as “reliable” as other structures that are explicitly in building codes.

While many reliability studies have been conducted on concrete and steel [2,3] and – to a lesser extent – timber structural systems [4], the seismic reliability of timber-based hybrid structures is still a novel field of research.

In this paper, we extend the application of the method by Li et al. [5] in determining the response surface database with polynomial functions by considering more uncertainties and analysis of variance (ANOVA). The objective of this study is to utilize response surface and importance sampling (IS) to estimate the seismic reliability index β of a novel timber-steel hybrid system called “Finding the Forest Through the Trees” (FFTT).

2. RESPONSE SURFACE DATABASE

2.1. Models of FFFT system

The FFFT system was introduced to the public in the Tall Wood Report [6]. The system utilizes engineered timber products such as Cross-Laminated-Timber (CLT) to resist gravity and lateral loads, with interconnecting steel beams to provide ductility for seismic demands.

Previous work investigated the non-linear dynamic response of this new structural concept [7, 8]. It is, however, deemed important to assess FFFT's seismic reliability to evaluate the influence of the structural input variables of interest for future performance-based design of this timber-steel hybrid system.

The reliability analysis presented herein is based on FFFT Option 1, which is designed for buildings up to 12 storeys and relies on CLT core walls with linked steel beams to provide lateral resistance. Glulam frames are utilized to resist gravity loads. Figure 1 shows the schematic of Option 1 of the FFFT system.

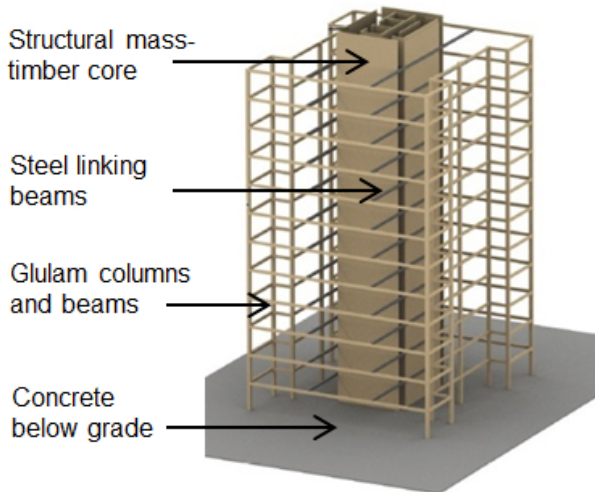


Figure 1: Schematic of Option 1 FFFT system [6]

The finite element models developed for the nonlinear dynamic analyses are similar to the numerical models previously developed in OpenSees to study Option 1 of the FFFT system under seismic loads. As there are various uncertainties taken into account when conducting

a reliability study, it was necessary to use more computationally efficient models. In lieu of a grid of 2D shell elements to model the CLT walls in the previous models [7], more efficient TwoNodeLink elements were used. These elements were modeled with three linear springs to provide equivalent axial, shear and bending stiffnesses. Figure 2 shows the schematic sketch of the simplified 2D model for one story of the FFFT system.

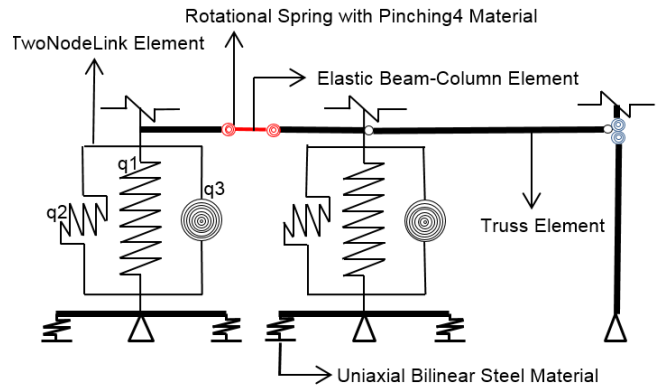


Figure 2: Schematic sketch of simplified 2D OpenSees model for 12 stories FFFT building

2.2. Uncertainties for Consideration

In seismic reliability analyses, uncertainty can be characterized as either 'aleatory' (stems from natural randomness and cannot be reduced) or 'epistemic' (stems from a fundamental lack of knowledge and can be reduced) [9]. In this study, aleatory uncertainty is accounted for in the record-to-record variability in the large suite of ground motions selected and their intensity. Epistemic uncertainty is captured through modeling variability in the structural properties such as weight and connection properties.

In this study, the 22 far-field earthquake ground motions considered in FEMA P695 [10] were selected as the ground motion record set and the intensity measure (IM) is represented by averaging the spectral acceleration over the period range of the models. Because the FFFT system was first proposed for Vancouver, BC, the 5% damped 2% in 50 year spectrum for Vancouver was chosen as the target spectrum to represent the seismic hazard.

First, all 22 individual far-field records are linearly scaled to the design response spectrum over the period range of the models. Then these ground motion records are further scaled to multiple intensity levels (25, 50, 100, 125, 150, 175, 200, 225 and 250% of the target spectrum). A period range from $0.2T_{low}$ to $1.5T_{high}$ was chosen, where T_{low} is the lowest fundamental period and T_{high} is the largest fundamental period of all of the models based on selected weight (mass) and hold-down stiffness level. Figure 3 shows the scaled response spectra of the 22 records for a 12 story FFTT system building designed with a ductility factor $R_d=3$.

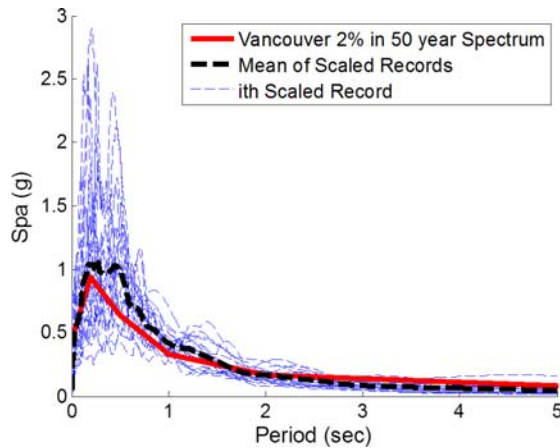


Figure 3: Scaled response spectra for 12 storey FFTT system

As hold-down solution for the FFTT system, the HSK (Holz-Stahl-Komposit) [11] system is chosen. Static tests on this system determined a connection stiffness in the range of 6.0×10^5 kN/m. To model this as a random variable, four hold-down stiffness levels ($2.0, 4.0, 6.0, 8.0 \times 10^5$ kN/m) are considered in this study. Three structural weight levels ($3.0, 4.0, 5.0$ kN/m²) were taken into account - the calculated mass of the structure is approximately 4.0 kN/m². The resulting period range of 0.5-4.8 seconds can be used to capture the elastic response, which is expected to govern inelastic displacements of all structural models.

Aside from the IM, building weight, hold-down stiffness, the uncertainty caused by the

bearing connection between steel beams and CLT panels is also taken into account. The steel beams are related to the system ductility factor as they are designed to yield and absorb seismic energy. A previous study [7] demonstrated that a properly-calibrated concentrated rotational spring model located at the beam-wall interface can efficiently capture the complete nonlinear behavior of the connection detail including steel yielding and timber crushing, as well as cyclic and in-cycle strength and stiffness degradation. Figure 4 illustrates the material model of this connection, calibrated to experimental tests [12] using the OpenSees Pinching4 material model.

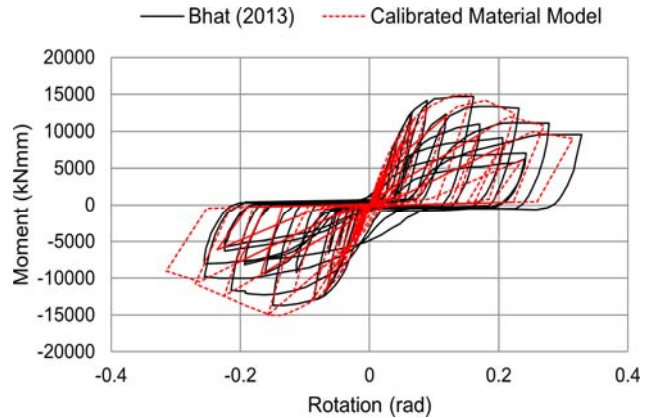


Figure 4: Calibration of steel-beam CLT panel connection [7]

To investigate the influence of the connection properties for the structural reliability, the fitted parameters are considered to be mean values from the test results. Variability is added as parameters k_2 and u_2 assumed to be perfectly correlated, with k_2 varying randomly across springs, while all other parameters are assumed deterministic and equal to the fitted values. The coefficient of variation of k_2 is assumed to be 0.2 from a similar study on wood shearwalls [4]. In this case, three different u_2 (0.13, 0.15 and 0.18 rad) and their corresponding k_2 values were selected to represent the uncertainty of the capping point. Figure 5 presents the general backbone curve of the piecewise linear hysteresis of this bearing connection.

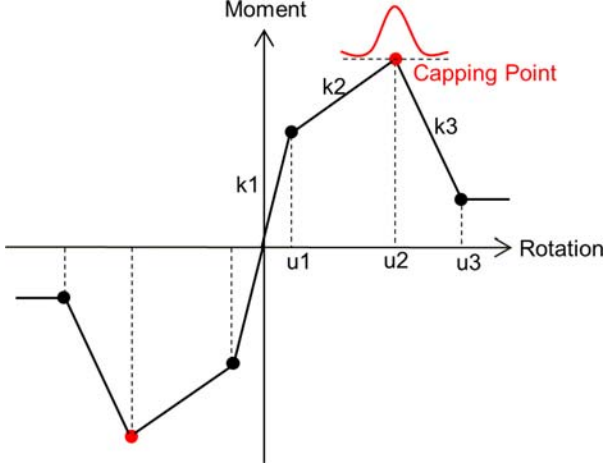


Figure 5: Piecewise linear hysteresis backbone curve

For the 12 storey design Option 1 of the FFTT system, buildings designed assuming three different R_d factors ($R_d = 3, 4$ and 5) are studied. For each individual design, the 22 ground motion suite with 10 different intensity levels, three structural weight levels, four hold-down stiffness levels and three capping point levels were considered. A simplifying assumption is made that the peak inter-storey drift corresponds to the damage in the FFTT system. In order to obtain the seismic response database, a total of 23,760 nonlinear dynamic analyses were run.

2.3. Polynomial function

In the seismic response database, it is possible to obtain the mean μ_Δ and standard deviation σ_Δ of the peak inter-storey drift response over the ground motion suite for each combination of defined variables. Herein, there are 360 sets of μ_Δ and σ_Δ for each ductility design values leading to 1,080 sets in total. For brevity, Table 1 provides a partial set of these statistical data of the peak inter-storey drift form the 12-storey building designed with $R_d=4$.

Fourth-order polynomial functions are used to fit the μ_Δ and σ_Δ of peak inter-storey drift over the domain of the four considered random variables (IM, structural weight, hold-down stiffness and capping point of the connection hysteresis loop).

Table 1: Statistical data of the peak inter-storey drift form the 12-storey building designed with $R_d=4$.

IM (%)	Weight (kN/m ²)	Stiffness (kN/m)	CP_u^* (rad)	μ_Δ (mm)	σ_Δ (mm)
25	3.0	200,000	0.18	11.4	3.2
50	5.0	600,000	0.15	24.3	5.5
75	4.0	400,000	0.13	33.2	7.5
100	3.0	600,000	0.18	36.9	8.2
125	4.0	800,000	0.18	48.7	10.4
150	3.0	600,000	0.18	52.5	12.6
175	5.0	400,000	0.15	76.6	19.2
200	4.0	800,000	0.18	78.8	22.6
225	5.0	800,000	0.15	94.4	26.5
250	4.0	600,000	0.13	100.7	30.9

* CP_u represents different u_2 of the capping point.

Equation (1) shows all possible components in the fitting polynomial function and all the coefficients of the equation can be obtained by minimizing the square errors between the actual response data and the fitted response surface.

$$\begin{aligned}
 \mu_\Delta(\sigma_\Delta) = & a + \sum_{i=1}^n b_i x_i + \sum_{i=1, i \neq j}^n c_{ij} x_i x_j + \sum_{i=1}^n d_i x_i^2 \\
 & + \sum_{i, j, k=1; i \neq j \neq k}^n e_{ijk} x_i x_j x_k + \sum_{i, j=1; i \neq j}^n f_{ij} x_i x_j^2 \\
 & + \sum_{i, j=1; i \neq j}^n g_{ij} x_i^2 x_j^2 + \sum_{i=1}^n h_i x_i^3 + \sum_{i, j, k, l=1; i \neq j \neq k \neq l}^n i_{ijkl} x_i x_j x_k x_l \\
 & + \sum_{i, j, k=1; i \neq j \neq k}^n j_{ijk} x_i^2 x_j x_k + \sum_{i, j=1; i \neq j}^n k_i x_i^3 x_j + \sum_{i=1}^n l_i x_i^4 \quad (1)
 \end{aligned}$$

As fourth-order polynomial functions are considered as fitted response surface and four variables are investigated, there are many components in this equation; however, not all of them have a critical contribution to the results. To simplify the equation and to determine the best regression from all possible combinations, the stepwise regression ANOVA selection method is used [13]. By considering this method, the fitted polynomial function is simplified, and it is ensured that all the components in the equation have a significant influence in the regression.

Equations (2) to (7) show all polynomial functions for the statistical data sets (mean and standard deviation) of the three 12-storey FFTT buildings with different ductility factors used for design. In these functions, x_1 represents the IM variable, x_2 represents the seismic weight variable, x_3 represents the hold-down stiffness variable and x_4 represents the capping point in the connection hysteresis loop.

From these regressions, it can be seen that there is no x_4 , which means that all the possible components involved with x_4 in the fourth-order polynomial response surface fitting function have already been eliminated by the ANOVA as the critical p -values of these components are bigger than the chosen significance ($\alpha=0.05$), then the null hypothesis of the no significance for these components are accepted.

The explanation that changing the location of the capping point in the wall-beam connection hysteresis loop has little influence for the peak inter-story drift of the FFTT system is because the capping point location in the hinge models only has an effect on the structure when the displacements are large enough to push the hinges past this point. Very few of the selected ground motions, even at high scaling levels, were intense enough to cause this displacement. Additionally, as seen in Figure 4, the slope of the strength loss past this point is very low.

Figure 6 shows one example of the predicted polynomial regression vs. the actual response for a 12-storey FFTT building model designed with $R_d=3$. Errors are relatively small and most data points are located near the 45° line, confirming the goodness-of-fit.

In order to evaluate the regression, Table 2 gives the R^2 and Adjusted- R^2 values of 12 storey FFTT systems designed with different ductility factors. From these values, it can be seen that the predicted polynomial response surface function fits very well with the actual data as both R^2 and adjusted R^2 very close to 1.

$$\begin{aligned} \mu_{\Delta 3} = & 29.53 + 29.20x_1 - 14.87x_2 - 1.09e^{-4}x_3 + 8.97x_1x_2 \\ & - 8.31e^{-5}x_1x_3 + 5.51e^{-5}x_2x_3 - 2.03x_1^2 + 1.85x_2^2 \\ & + 1.81e^{-10}x_3^2 + 1.95e^{-5}x_1x_2x_3 - 1.66x_1^2x_2 - 1.93e^{-6}x_1^2x_3 \\ & - 0.60x_1x_2^2 + 5.49e^{-11}x_1x_3^2 - 7.09e^{-6}x_2^2x_3 - 6.89e^{-11}x_2x_3^2 \\ & + 1.75x_1^3 - 7.75e^{-17}x_3^3 + 1.27e^{-6}x_1^2x_2x_3 - 1.12e^{-6}x_1x_2^2x_3 \\ & - 1.15e^{-11}x_1x_2x_3^2 + 7.17e^{-12}x_2^2x_3^2 + 1.52e^{-17}x_2x_3^3 \quad (2) \end{aligned}$$

$$\begin{aligned} \sigma_{\Delta 3} = & 30.68 - 20.51x_1 - 15.82x_2 - 1.84e^{-5}x_3 + 14.04x_1x_2 \\ & + 25.47e^{-5}x_1x_3 + 1.92e^{-5}x_2x_3 - 19.20x_1^2 + 1.92x_2^2 \\ & - 3.50e^{-11}x_3^2 - 3.93e^{-5}x_1x_2x_3 + 9.64x_1^2x_2 - 8.43e^{-7}x_1^2x_3 \\ & - 1.12x_1x_2^2 + 2.90e^{-11}x_1x_3^2 - 3.15e^{-6}x_2^2x_3 + 8.39e^{-12}x_2x_3^2 \\ & + 1.60x_1^3 - 1.47x_1^2x_2^2 + 3.28e^{-6}x_1^2x_2x_3 + 4.67e^{-6}x_1x_2^2x_3 \\ & - 5.73e^{-12}x_1x_2x_3^2 - 2.64e^{-6}x_1^3x_3 \quad (3) \end{aligned}$$

$$\begin{aligned} \mu_{\Delta 4} = & 21.73 + 40.92x_1 - 13.42x_2 - 8.25e^{-5}x_3 + 12.97x_1x_2 \\ & - 1.67e^{-4}x_1x_3 + 4.47e^{-5}x_2x_3 - 4.32x_1^2 + 1.64x_2^2 \\ & + 2.15e^{-10}x_3^2 + 3.67e^{-5}x_1x_2x_3 - 7.87x_1^2x_2 + 2.73e^{-5}x_1^2x_3 \\ & - 1.20x_1x_2^2 + 8.22e^{-11}x_1x_3^2 - 5.16e^{-6}x_2^2x_3 - 7.81e^{-11}x_2x_3^2 \\ & + 5.57x_1^3 - 1.13e^{-16}x_3^3 + 0.59x_1^2x_2^2 - 9.70e^{-7}x_1^2x_2x_3 \\ & - 7.94e^{-12}x_1^2x_3^2 - 2.37e^{-6}x_1x_2^2x_3 - 1.28e^{-11}x_1x_2x_3^2 \\ & + 6.36e^{-12}x_2^2x_3^2 + 0.80x_1^3x_2 - 3.24e^{-6}x_1^3x_3 + 2.5e^{-17}x_2x_3^3 \\ & - 0.94x_1^4 \quad (4) \end{aligned}$$

$$\begin{aligned} \sigma_{\Delta 4} = & 34.23 - 53.91x_1 - 21.39x_2 + 3.41e^{-5}x_3 + 36.58x_1x_2 \\ & - 3.34e^{-5}x_1x_3 + 4.62e^{-6}x_2x_3 + 8.55x_1^2 + 3.01x_2^2 \\ & - 6.12e^{-11}x_3^2 - 1.70e^{-5}x_1x_2x_3 - 3.41x_1^2x_2 + 2.06e^{-5}x_1^2x_3 \\ & - 4.40x_1x_2^2 + 6.45e^{-11}x_1x_3^2 - 2.74e^{-6}x_2^2x_3 + 1.52e^{-11}x_2x_3^2 \\ & - 3.63x_1^3 + 4.14e^{-6}x_1x_2^2x_3 - 1.48e^{-11}x_1x_2x_3^2 + 0.89x_1^3x_2 \\ & - 5.18e^{-6}x_1^3x_3 + 0.71x_1^4 \quad (5) \end{aligned}$$

$$\begin{aligned} \mu_{\Delta 5} = & 13.12 + 29.67x_1 - 8.02x_2 - 2.68e^{-5}x_3 + 21.30x_1x_2 \\ & - 2.03e^{-4}x_1x_3 + 7.09e^{-7}x_2x_3 + 5.71x_1^2 + 0.98x_2^2 \\ & + 2.54e^{-10}x_3^2 + 4.85e^{-5}x_1x_2x_3 - 13.03x_1^2x_2 + 3.80e^{-5}x_1^2x_3 \\ & - 2.64x_1x_2^2 + 7.88e^{-11}x_1x_3^2 + 1.18e^{-6}x_2^2x_3 - 5.21e^{-11}x_2x_3^2 \\ & + 4.27x_1^3 - 2.21e^{-16}x_3^3 + 1.28x_1^2x_2^2 - 2.61e^{-6}x_1^2x_2x_3 \\ & - 1.46e^{-11}x_1^2x_3^2 - 2.43e^{-6}x_1x_2^2x_3 - 2.03e^{-11}x_1x_2x_3^2 \\ & + 1.04x_1^3x_2 - 2.63e^{-6}x_1^3x_3 + 3.13e^{-17}x_1x_3^3 + 4.49e^{-17}x_2x_3^3 \\ & - 0.93x_1^4 \quad (6) \end{aligned}$$

$$\begin{aligned} \sigma_{\Delta 5} = & 52.19 - 103.16x_1 - 32.01x_2 + 5.83e^{-5}x_3 + 64.30x_1x_2 \\ & - 7.95e^{-5}x_1x_3 - 2.68e^{-8}x_2x_3 + 33.97x_1^2 + 4.47x_2^2 \\ & - 9.31e^{-11}x_3^2 - 7.86e^{-6}x_1x_2x_3 - 16.57x_1^2x_2 + 3.25e^{-5}x_1^2x_3 \\ & - 7.92x_1x_2^2 + 1.07e^{-10}x_1x_3^2 - 3.16e^{-6}x_2^2x_3 + 2.40e^{-11}x_2x_3^2 \\ & - 5.56x_1^3 + 1.40x_1^2x_2^2 + 4.39e^{-6}x_1x_2^2x_3 - 2.67e^{-11}x_1x_2x_3^2 \\ & + 1.55x_1^3x_2 - 9.07e^{-6}x_1^3x_3 + 1.05x_1^4 \quad (7) \end{aligned}$$

Table 2: The fitness of the polynomial function

Ductility Factor(R_d)	Statistic Data	R2	Adjusted R2
3	Mean ($\mu_{\Delta 3}$)	0.999	0.999
	StDev ($\sigma_{\Delta 3}$)	0.995	0.995
4	Mean ($\mu_{\Delta 4}$)	0.999	0.999
	StDev ($\sigma_{\Delta 4}$)	0.991	0.990
5	Mean ($\mu_{\Delta 5}$)	0.999	0.999
	StDev ($\sigma_{\Delta 5}$)	0.990	0.989

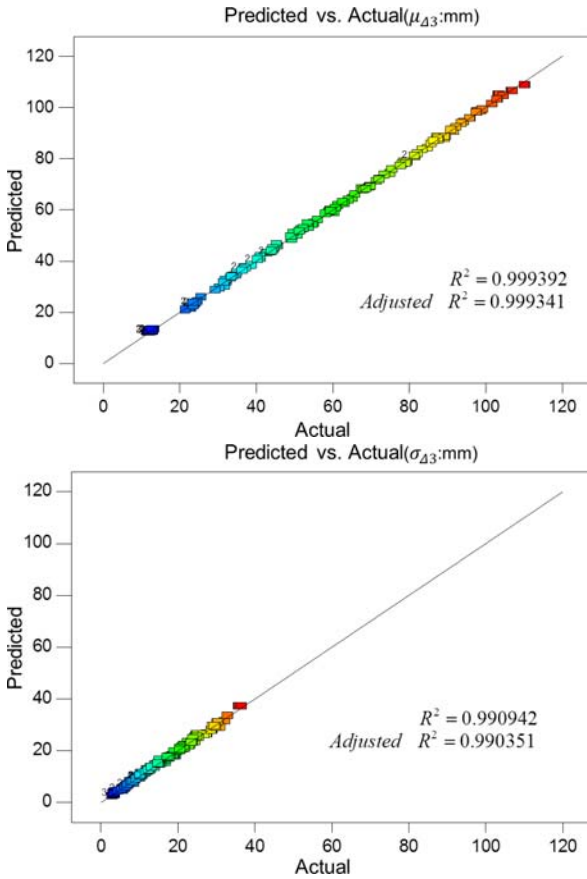


Figure 6: Predicted mean and standard deviation of the polynomial regression vs. the actual response for 12-storey FFTT building with $R_d=3$

As the 4D response surface of the obtained polynomial functions is difficult to draw, Figure 7 gives an example of a 3D response surface of peak inter-storey drift mean and standard deviation for the 12-storey FFTT building with $R_d=4$ and fixed stiffness ($x_3 = 400,000\text{kN/m}$).

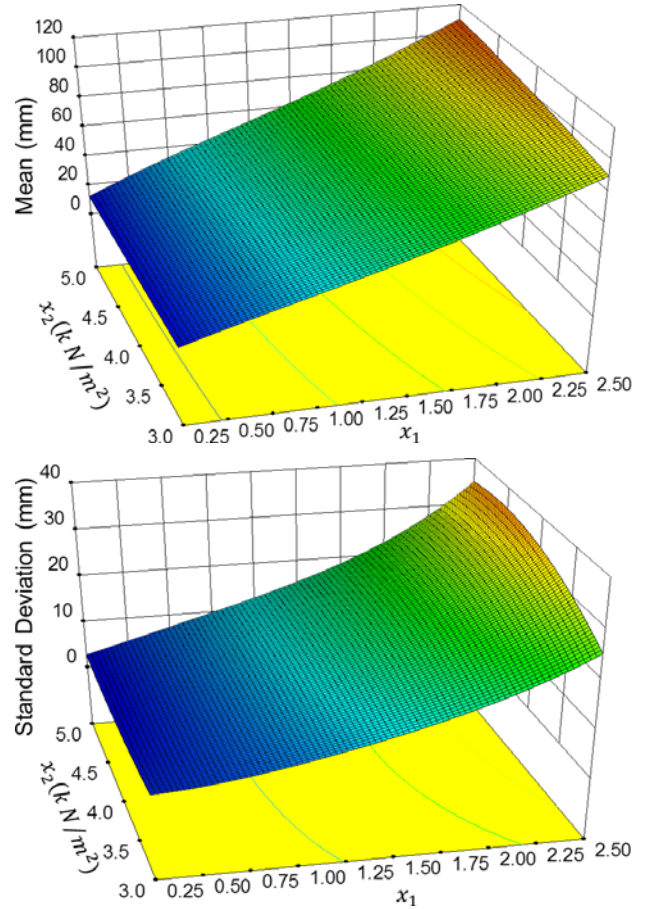


Figure 7: Polynomial response surface of peak inter-storey drift mean (top) and standard deviation (bottom) for 12-storey FFTT building with $R_d=4$ and hold-down stiffness $x_3=400,000\text{kN/m}$

3. RELIABILITY ANALYSIS

3.1. Performance function

Through performance-based seismic design, the extent of structural damage can be related to performance in seismic events and design methodologies to mitigate future losses can be developed. For simplification, performance – as a predictor of total structural damage – is related to peak inter-storey drift.

Based on the obtained polynomial function of the μ_{Δ} and σ_{Δ} for peak inter-storey drift over the domain of the considered random variables, the performance function, Equation (8), can be formulated by using the assumption that the peak inter-storey drift follows a lognormal distribution [5]:

$$G = \delta - \Delta = \zeta H - \frac{\mu_{\Delta}}{\sqrt{1 + \nu_{\Delta}^2}} \exp(R_N \sqrt{\ln(1 + \nu_{\Delta}^2)}) \quad (8)$$

where δ is the inter-storey drift capacity of the building (equal to the drift ratio limit ζ times the storey building height H); Δ is the peak inter-storey demand which involves the characteristic of the intervening random variables (it can be obtained by transforming equation (8)); μ_{Δ} is the mean of the peak inter-storey drift demand; ν_{Δ} is the coefficient of variation ($\sigma_{\Delta}/\mu_{\Delta}$); R_N is the standard normal variate $R_N(0,1)$; and μ_{Δ} and σ_{Δ} for the FFTT system with different ductility designs are given by Equations (2) to (7).

3.2. Reliability results

Once the explicit performance function Equation (8) and the probability distributions for the considered variables are obtained, the reliability index β can be estimated by first order reliability method (FORM) or IS simulation.

Herein, the *Rt* software was used to conduct the reliability index calculation [14]. For the 12 storey FFTT systems designed with different ductility factors, the ground motion intensity measure (x_1) is assumed to follow a lognormal distribution, with a mean value equal 100% and with COV of 0.6 [5]; the seismic weight (x_2) and the hold-down stiffness (x_3) are both assumed to follow a lognormal distribution with COV of 0.1. The variation of the capping point in connection hysteresis loop (x_4) wasn't considered as it is not significant in the polynomial function.

Three different performance expectations are considered: inter-storey drift limit of 1.5% for immediate occupancy (*IO*); 2.5% for life safety (*LS*) and 4% for collapse prevention (*CP*) [15]. Table 3 gives the FORM and IS results of the reliability index for the three ductility designs and performance expectations with the mean of weight equal 4.0kN/m² and mean of stiffness equal 600,000kN/m.

Table 3: Reliability index with three ductility designs for three performance expectations (weight mean =4.0kN/m² and stiffness mean=600,000kN/m)

R_d	β					
	<i>IO</i>		<i>LS</i>		<i>CP</i>	
	FORM	IS	FORM	IS	FORM	IS
3	0.45	0.50	1.43	1.46	2.19	2.20
4	0.47	0.50	1.41	1.45	2.17	2.29
5	0.46	0.50	1.39	1.42	2.12	2.23

Figures 8 and 9 show the effects of weight and stiffness respectively for the reliability index of the FFTT with $R_d=5$ in *LS*. For brevity, only the results for $R_d=5$ and in *LS*, are given; for the designs using other ductility factors in other performance expectations, similar trends were observed.

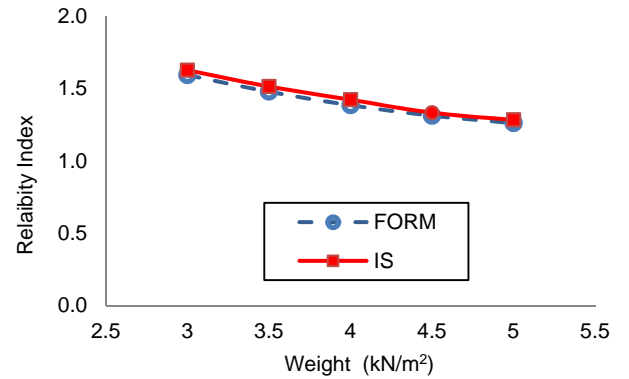


Figure 8: Reliability index in *LS* for FFTT with $R_d=5$ and hold-down stiffness $x_3=600,000$ kN/m

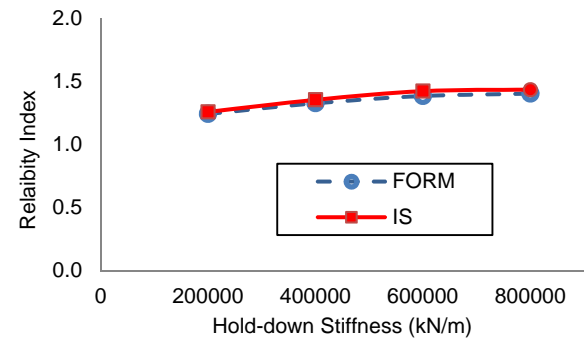


Figure 9: Reliability index in *LS* for FFTT with $R_d=5$ and structural weight $x_2=4.0$ kN/m²

4. CONCLUSION

This paper presented seismic reliability analyses of the FFTT system as an example of novel timber-steel hybrid structural systems. An efficient response surface method together with FORM and IS simulation was developed to estimate the structural reliability. By using the stepwise ANOVA method, any given number of intervening random variables can be taken into account without adding the complication of the response polynomial function while ensuring that all the components in regression are significant and increasing the accuracy of the fitted function. The results can be summarized as follows:

- (1) Structural weight (mass) and stiffness have significant influence on failure probability: β increased with the decrease of the weight (mass) and increase of the hold-stiffness.
- (2) The FORM and IS gave very similar β with the IS results being slightly higher.
- (3) The ductility design values didn't have a strong influence on the failure probability.
- (4) For three performance expectations, β varies significantly. β for IO is relatively low ($\beta \approx 0.50$, probability of exceedance, $P_e \approx 31\%$) due to the strict requirements for IO. However, β is acceptable for LS and CP ($\beta \approx 1.44$ and 2.24 , $P_e \approx 7.5\%$ and 1.2% , respectively).

5. REFERENCES

- [1] Haukaas, T. (2008). Unified reliability and design optimization for earthquake engineering. *Probabilistic Engineering Mechanics*, 23,471–481.
- [2] Sasani, M., and Der Kiureghian, A. (2001). Seismic fragility of RC structural walls: Displacement approach. *Journal of Structural Engineering*, 127(2),219–228.
- [3] Wen, Y. K., Foutch, D. A., Eliopoulis, D., and Yu, C. Y. (1994a). Seismic reliability of current code procedures for steel buildings. Proc., 5th National Conf. on Earthquake Engineering, Chicago, USA.
- [4] Ceccotti, A., and Foschi, R. O. (1998). Reliability assessment of wood shear walls under earthquake excitation. Proc. 3rd Int. Conf. on Computational Structural Mechanics, Thera-Santorini, Greece.
- [5] Li, M., Lam, F., Foschi, R. O., Nakajima, S., and Nakagawa, T. (2012). Seismic performance of post-and-beam timber buildings II: reliability evaluations. *Journal of Wood Science*. 58(2): 135-143.
- [6] Green M., and Karsh J.E. (2012). Tall Wood-The Case for Tall Wood Buildings. Wood Enterprise Coalition. Vancouver, Canada.
- [7] Fairhurst, M., Zhang, X. and Tannert, T. (2014). Nonlinear Dynamic Analysis of a Novel Timber-Steel Hybrid System. Proc., World Conference on Timber Engineering, Quebec City, Canada.
- [8] Zhang, X., Fairhurst, M. and Tannert, T. (2014). Ductility Estimation for a Novel Timber-Steel-Hybrid System. Submitted to *Journal of Structural Engineering*.
- [9] Kiureghian, A. D., & Ditlevsen, O. (2009). Aleatory or Epistemic? Does it Matter?. *Structural Safety*, 31(2), 105-112.
- [10] FEMA (2009). Recommended Methodology for Quantification of Buildings System Performance and Response Parameters, Report No. FEMA P-695, Prepared by Applied Technology Council, Federal Emergency Management Agency, Washington, USA.
- [11] Bathon, L., Bletz-Mühldorfer, O., Schmidt, J., Diehl, F. (2014). Fatigue Design of Adhesive Connections Using Perforated Steel Plates. Proc. World Conference on Timber Engineering, Quebec City, Canada.
- [12] Bhat, P. (2013). Experimental Investigation of Connection for the FFTT, A Timber-steel Hybrid System. MASC thesis, University of British Columbia, Vancouver, Canada.
- [13] Montgomery, D.C., and Runger, G.C. (2003). Applied statics and probability for engineers. Wiley&Sons, NewYork, USA.
- [14] Mahsuli, M., and Haukaas, T. (2013). "Computer Program for Multimodel Reliability and Optimization Analysis." *Journal of Computing in Civil Engineering*, 27(1), 87–98.
- [15] Pei, S., Popovski, M., and van de Lindt, J.W. (2013). Analytical Study on Seismic Force Modification Factors for Cross-laminated Timber Building for NBCC. *Canadian Journal of Civil Engineering*, 40(9): 887-896.